

## Studies of ${}^6\text{Li}$ -NMR properties in different salt solutions in low magnetic fields

A. Gordji-Nejad <sup>a,\*</sup>, J. Colell <sup>b</sup>, S. Glögler <sup>b,c</sup>, B. Blümich <sup>b</sup>, S. Appelt <sup>a,b</sup>

<sup>a</sup> Central Institute for Electronics, Research Center Jülich, D-52425 Jülich, Germany

<sup>b</sup> Institute for Technical Chemistry and Macromolecular Chemistry, RWTH Aachen University, D-52056 Aachen, Germany

<sup>c</sup> II. Institute of Physics, RWTH Aachen University, D-52074 Aachen, Germany

### ARTICLE INFO

#### Article history:

Received 9 August 2011

Revised 16 September 2011

Available online 7 October 2011

#### Keywords:

Low-field

Lithium-6

Relaxation

### ABSTRACT

In this article we report the longitudinal relaxation times ( $T_1$ ) of various  ${}^6\text{Li}$  salts ( ${}^6\text{LiI}$ ,  ${}^6\text{LiCl}$  and  ${}^6\text{LiNO}_3$ ) in  $\text{D}_2\text{O}$  and  $\text{H}_2\text{O}$ , measured in low magnetic fields ( $B_0 = 3.5$  mT). This investigation serves the purpose of clarifying the relaxation behavior of different  ${}^6\text{Li}$  solutions and different concentrations. The measurement were undertaken to establish a framework for future applications of hyperpolarized  ${}^6\text{Li}$  in medical imaging, biological studies and investigations of lithium ion batteries. Time will pass during the transport of hyperpolarized lithium ions to the sample, which leads to a polarization loss. In order to store polarization as long as possible, it is necessary to examine which  ${}^6\text{Li}$  salt solution has the longest relaxation time  $T_1$ . Longitudinal relaxation times of  ${}^6\text{Li}$  salts in  $\text{D}_2\text{O}$  and  $\text{H}_2\text{O}$  were investigated as a function of concentration and the most extended  $T_1$  was found for  ${}^6\text{LiI}$  in  $\text{D}_2\text{O}$  and  $\text{H}_2\text{O}$ . In agreement with the theory the relaxation time  $T_1$  of all  ${}^6\text{Li}$  salts increase with decreasing concentration. In the case of  ${}^6\text{LiI}$  in  $\text{H}_2\text{O}$  an inverse behavior was observed. We assume that the prolonged  $T_1$  times occur due to formation of  ${}^6\text{LiOH}$  upon the solution of  ${}^6\text{LiI}$  in  $\text{H}_2\text{O}$ , which settles as a precipitate. By diluting the solution, the precipitate continuously dissolves and approaches  $T_1$  of  ${}^6\text{LiOH}$  ( $T_1 \sim 28$  s), leading to a shorter  $T_1$  relaxation time.

© 2011 Elsevier Inc. All rights reserved.

### 1. Introduction

Nuclear Magnetic Resonance (NMR) [1–4] is a successful method for non-destructive investigation of materials and biological systems [5–7]. The main problem of NMR is the small signal-to-noise ratio (SNR) due to the very low polarization degree of the nuclear spins in magnetic fields ( ${}^1\text{H}$ -polarization degree  $P = 3 \times 10^{-6}$  at  $B_0 = 1$  T). This complicates the measurement of NMR spectra by using mobile spectrometers that operate at low magnetic fields. Especially, the SNR is very small for rare nuclei such as  ${}^{13}\text{C}$ ,  ${}^{29}\text{Si}$ ,  ${}^{129}\text{Xe}$  and  ${}^6\text{Li}$ , which are essential for many applications in materials science and medicine [8].  ${}^6\text{Li}$  plays a crucial role in brain chemistry and cases of clinical depression have been reported related to malnutrition and lithium deficiency.

Hyperpolarization technology such as SEOP [9,10], DNP [8,11–13], SPINOE [14,15], and PHIP [16–18] provide a suitable method to increase the SNR. The development and advancement of this technology has opened up many new applications that enriched the field of medical technology, biology, chemistry and physics [8,19,20]. Consequently, optimizing and extending this technology has moved more and more into the focus of scientific interest in recent years.

Among the rare nuclei the  ${}^6\text{Li}$  nucleus is a promising sensor to study transport phenomena in biological systems (e.g. the brain) and membranes (e.g., Li-ion battery). For example, it has recently been shown that hyperpolarized  ${}^6\text{Li}$  can be used as a contrast agent for imaging in rat brains [8]. Since in low magnetic fields susceptibility artifacts become smaller, low field NMR should be advantageous to study dynamics in Li ion batteries, especially if they contain metal parts. Furthermore, at lower magnetic fields achieving the high field homogeneities over large samples is less problematic and imaging artifacts that arise when using frequency encoded images are removed due to vanishing chemical shift differences. The difference in relaxation times of free lithium and chemically bound lithium within a medium will offer extremely high contrasts in both  $T_1$  and  $T_2$  weighted images, further empowering low field approach.

For nuclei with spin quantum number  $I > 1/2$ , additional relaxation pathways such as quadrupolar interaction leads to polarization loss. In the case of  ${}^6\text{Li}$  ( $I_{6\text{Li}} = 1$ ), due to the low quadrupole moment of  $Q({}^6\text{Li}) = -8 \times 10^{-28}$  cm<sup>2</sup> and small gyromagnetic ratio  $\gamma^6\text{Li} = 6.266$  MHz/T it possesses a long relaxation time  $T_1$ , which is very important for NMR and MRI measurements. Hence long longitudinal relaxation times of diluted  ${}^6\text{Li}$  in  $\text{D}_2\text{O}$  up to 179 s have been reported [8].

However due to the small gyromagnetic ratio and the low natural abundance (7.42%),  ${}^6\text{Li}$ -NMR at low magnetic fields is extremely difficult. A theoretical study shows that it is possible to

\* Corresponding author.

E-mail address: [ali.gordji@post.rwth-aachen.de](mailto:ali.gordji@post.rwth-aachen.de) (A. Gordji-Nejad).

measure  ${}^6\text{Li}$  ions in the mT range, provided they are hyperpolarized prior to the measurement [22]. Here, we will demonstrate that NMR measurements of  ${}^6\text{Li}$  in the kHz range are possible by thermal pre-polarization of enriched  ${}^6\text{Li}$  ions in a 2 T Halbach-magnet.

This article deals with the study of  ${}^6\text{Li}$  ions in various fluids using nuclear magnetic resonance in the mT range. The purpose of this investigation was to study the relaxation effects such as dipole–dipole and quadrupolar interaction in the low field regime. Moreover since in the kHz regime the dipole–dipole rate is not depending on the Larmor frequency, the dipole rate equation simplifies and depends mainly on the correlation time  $\tau_c$ .

Regarding to the environment, the relaxation time depends to the magnetic or nonmagnetic nuclei that surrounds the  ${}^6\text{Li}$ . In the case of solvated  ${}^6\text{Li}$  salts in  $\text{H}_2\text{O}$  and  $\text{D}_2\text{O}$  the  ${}^6\text{Li}$  is surrounded by magnetic nuclei such as protons and deuterons. According to the relaxation theory the spin–lattice relaxation rate  $1/T_1$  is:

$$\frac{1}{T_1} = \gamma_{\text{Li}}^2 (\overline{B_x^2} + \overline{B_y^2}) \frac{\tau_0}{1 + \omega_0^2 \tau_0^2} \quad (1)$$

$\gamma_{\text{Li}}$  is the gyromagnetic ratio of  ${}^6\text{Li}$ ,  $B_x$  and  $B_y$  are the field fluctuation of the components of the  $B$  field,  $\tau_0$  is the correlation time and  $\omega_0$  the Larmor frequency. In high field and solid state  $\omega_0$  and  $\tau_0$  is high compared to liquid state in low field, hence very long relaxation time may occur in solid state.

Since the short correlation limit is valid in liquids states, the relaxation rate depends mainly to the dipole–dipole and quadrupole correlation time  $\tau_c$  and  $\tau_q$ . The short correlation time in the liquid state reduces the effects of the dipole–dipole and the quadrupolar interaction to mathematically simpler expressions and leads to an extension of the relaxation time [23].

To determine in which salt solutions the  ${}^6\text{Li}$  has the longest relaxation time, the  ${}^6\text{Li}$ -ions of different aqueous ( $\text{H}_2\text{O}$  and  $\text{D}_2\text{O}$ ) salt solutions ( ${}^6\text{LiI}$ ,  ${}^6\text{LiNO}_3$ ,  ${}^6\text{LiCl}$ ,  ${}^6\text{LiOH}$ ,  ${}^6\text{LiOD}$ ) were first pre-polarized in a 2 T Halbach-magnet and the  ${}^6\text{Li}$ -NMR signal was measured in low-field at  $B_0 = 3.5$  mT. The  ${}^6\text{LiCl}$  compound was chosen because of its low toxicity and its use as a contrast agent has been reported [8]. To study the anion influence other highly soluble ( ${}^6\text{LiI}$ ,  ${}^6\text{LiNO}_3$ ) salts have been used. As the  ${}^6\text{LiOH}$  is the reaction product of  ${}^6\text{Li}$  with water it is relevant to study the behavior of aqueous hydroxide solutions, as biological processes occur in those environments. It turns out that  ${}^6\text{LiI}$  salt in diluted deuterated water has the longest relaxation time ( $T_1 \sim 177$  s) of all samples.

Subsequently, the  $T_1$  relaxation times of various  ${}^6\text{Li}$  salt solutions at different concentrations are compared and the relaxation properties are studied. According to the expectation, the dilution of the  ${}^6\text{Li}$  samples leads to an extension of the  ${}^6\text{Li}$   $T_1$  relaxation time. Only dissolved  ${}^6\text{LiI}$  in water shows an anomalous behavior. The  ${}^6\text{Li}$  relaxation time  $T_1$  gets shorter with decreasing concentration. This is related to the conversion reaction of  ${}^6\text{LiI}$  in water to sparingly soluble  ${}^6\text{LiOH}$ .

## 2. Experimental section

### 2.1. Sample preparation

First, the  ${}^6\text{Li}$  (99%) NMR signal of a saturated solution  ${}^6\text{LiCl}$  in  $\text{D}_2\text{O}$  is measured.  $\text{D}_2\text{O}$  was selected because the  ${}^6\text{Li}$   $T_1$  time in  $\text{D}_2\text{O}$  is longer compared to  $\text{H}_2\text{O}$  due to the reduced dipole–dipole and quadrupolar interaction. Thus, the loss of the polarization of  ${}^6\text{Li}$  during the transport to the NMR device can be reduced.

To prepare the saturated solution samples,  $m_{\text{LiCl}} = 0.416$  g of  ${}^6\text{LiCl}$  ( $c_{\text{LiCl}} = 20.05$  mol/L) salt was dissolved in  $\text{D}_2\text{O}$  and  $\text{H}_2\text{O}$  (0.5 mL). This corresponds to a  ${}^6\text{Li}$  spin density of  $[{}^6\text{LiCl}] = 6.03 \times 10^{21} \text{ cm}^{-3}$ . To study the  $T_1$  behavior upon dilution, two additional  ${}^6\text{LiCl}$  samples were prepared with  ${}^6\text{LiCl}$  ( $c_{\text{LiCl}} = 16.96$  mol/L) and  ${}^6\text{LiCl}$  ( $c_{\text{LiCl}} = 9.75$  mol/L).

${}^6\text{LiNO}_3$  ( $c_{\text{LiNO}_3} = 7.67$  mol/L,  $[{}^6\text{LiNO}_3] = 2.3 \times 10^{21} \text{ cm}^{-3}$ ) and  ${}^6\text{LiI}$  ( $c_{\text{LiI}} = 11.3$  mol/L,  $[{}^6\text{LiI}] = 3.4 \times 10^{21} \text{ cm}^{-3}$ ) were dissolved in the same procedure in 0.5 mL  $\text{D}_2\text{O}$  and  $\text{H}_2\text{O}$  to obtain saturated solutions and two dilutions of both samples ( ${}^6\text{LiNO}_3$  ( $c_{\text{LiNO}_3} = 6.35$  - mol/L), ( $c_{\text{LiNO}_3} = 5.00$  mol/L) and  ${}^6\text{LiI}$  ( $c_{\text{LiI}} = 7.67$  mol/L), ( $c_{\text{LiI}} = 5.50$  - mol/L) were prepared.

### 2.2. NMR spectroscopy

The sample is first pre-polarized in a 2 T Halbach-magnet. After the premagnetization, the sample is transported by hand into the measuring resonator which is situated in the center of the  $B_0$  coil (transport time  $\sim 1$  s). The  $B_0$  coil consists of a 2-piece solenoid with 3 ppm  $B_0$  homogeneity. The current ( $I = 5.357$  A) that is required for the  $B_0$  field is delivered from a high-precision power supply (0–10 A). The current stability is a few ppm over several minutes. The NMR signal is measured at  $B_0 = 3.5$  mT ( $\nu_{\text{Li}} = 20.66$  kHz) after a  $(\pi/2)$  excitation pulse (Fig. 1) [21].

## 3. Results and discussion

The  ${}^6\text{Li}$  signal-to-noise ratio (SNR) of  ${}^6\text{LiCl}$  in  $\text{D}_2\text{O}$  is  $\text{SNR} = 3.6$  (Fig. 2). A comparison with a theoretically calculated value ( $\text{SNR} = 8.6$ ) shows a  $\sim 2.3$ -fold lower SNR. The measured signal has a line width of  $\Delta\nu = 0.3$  Hz, the frequency offset is  $\Delta\nu_{\text{off}} = 56$  Hz. Even for  ${}^6\text{LiNO}_3$  ( $\text{SNR} = 2.1$ ) and  ${}^6\text{LiI}$  ( $\text{SNR} = 1.7$ ), both  ${}^6\text{Li}$  signals are clearly visible. However, they are lower than the  ${}^6\text{LiCl}$  signal. The SNR for  ${}^6\text{LiNO}_3$  is slightly higher than expected. This is because the preamplifier of the setup has a RMS noise between 100 and 140 mV, which leads to slight inconsistencies in calculated SNR upon comparison with the spin density especially for weak signals.

To prove whether a  ${}^6\text{Li}$  in  $\text{H}_2\text{O}$  can be measured or not, analogous saturated solutions of  ${}^6\text{LiI}$ ,  ${}^6\text{LiNO}_3$  and  ${}^6\text{LiCl}$  in  $\text{H}_2\text{O}$  are investigated. It turned out that the relaxation time of the highly

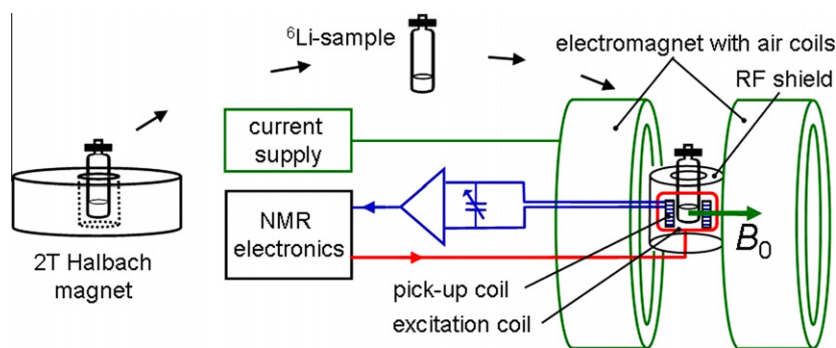
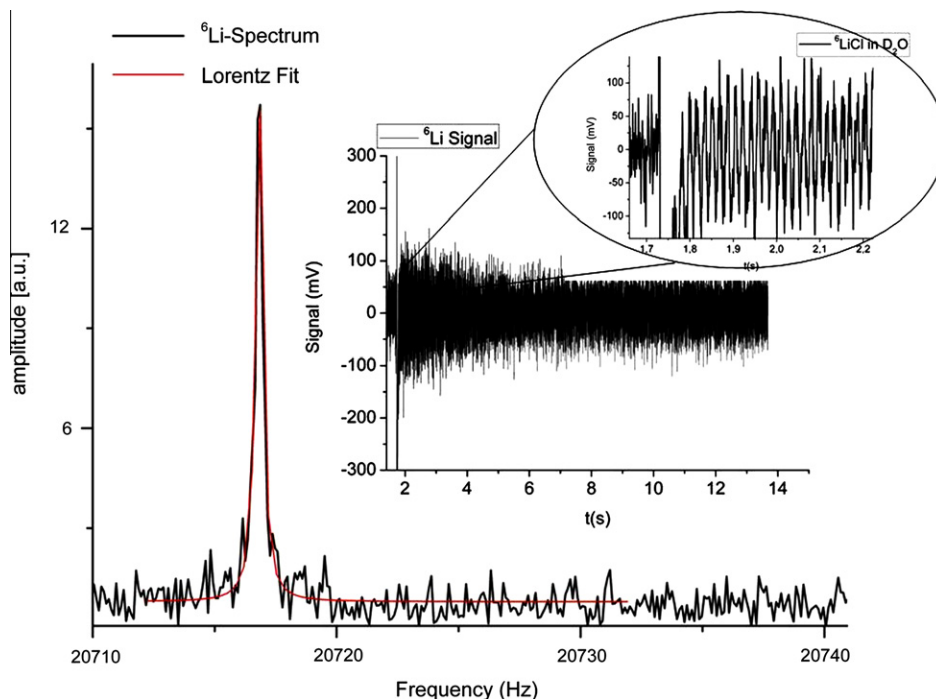
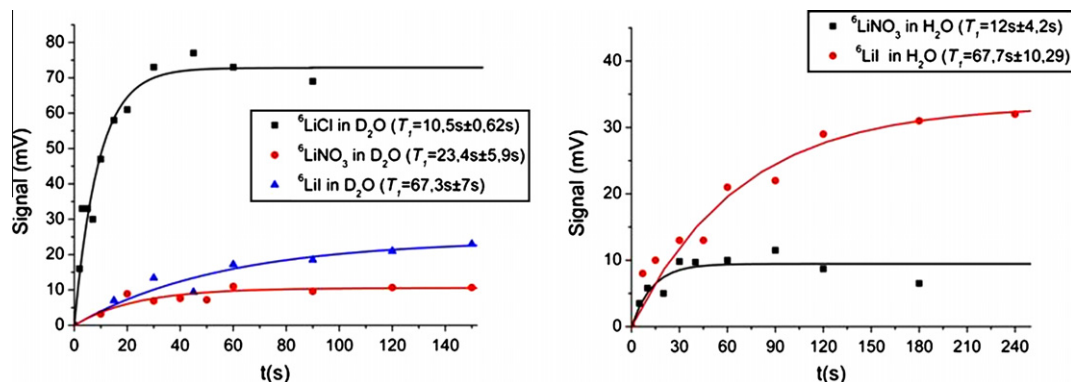


Fig. 1. Schematic presentation of the experiment: The NMR setup with power supply and NMR electronics as well as sample pre-polarization and transport is depicted [21].



**Fig. 2.** The  ${}^6\text{Li}$  spectrum of a saturated  ${}^6\text{LiCl}$  solution in  $\text{D}_2\text{O}$  at  $B_0 = 3.5$  mT (20.66 kHz). The  $S/N$  equals 3.6. Left: Fourier-transformed frequency spectrum with a line width of  $\Delta\nu = 0.3$  Hz.



**Fig. 3.**  $T_1$ -relaxation time of  ${}^6\text{LiCl}$  ( $T_1 = 10.5$  s),  ${}^6\text{LiNO}_3$  ( $T_1 = 23.4$  s) and  ${}^6\text{LiI}$  ( $T_1 = 67.3$  s) in  $\text{D}_2\text{O}$  (left).  $T_1$ -relaxation time of  ${}^6\text{LiNO}_3$  ( $T_1 = 12$  s) and  ${}^6\text{LiI}$  ( $T_1 = 67.7$  s) in  $\text{H}_2\text{O}$  (right).

concentrated  ${}^6\text{LiCl}$  solution is shorter than the transportation time from the Halbach-magnet to the NMR device ( $\sim 1$  s), which leads to a signal loss. Otherwise it is possible to measure the  ${}^6\text{Li}$  signal from  ${}^6\text{LiNO}_3$  ( $\text{SNR} \sim 2$ ) and  ${}^6\text{LiI}$  ( $\text{SNR} = 1.4$ ) in  $\text{H}_2\text{O}$ .

After it has been shown that thermally pre-polarized  ${}^6\text{Li}$  can be measured even at low magnetic fields ( $B_0 = 3.5$  mT), the question arises which of the  ${}^6\text{Li}$ -salt samples has the longest  $T_1$  relaxation time, since this is essential for the purpose to store the hyperpolarized  ${}^6\text{Li}$  and transport it to the NMR device. The  $T_1$  relaxation times are determined by the saturation recovery method, while in this case the evolution time  $\tau$  is replaced by a polarization time in the Halbach-magnet. This procedure is repeated with increasing time intervals until the saturated magnetization is reached.

In the following, results of  $T_1$  measurements for different saturated  ${}^6\text{Li}$  salt solutions in  $\text{D}_2\text{O}$  and  $\text{H}_2\text{O}$  will be discussed. We obtained the following relaxation times  ${}^6\text{LiCl}$ :  $T_1 = 10.5$  s;  ${}^6\text{LiNO}_3$ :  $T_1 = 23.4$  s and  ${}^6\text{LiI}$ :  $T_1 = 67.3$  s in  $\text{D}_2\text{O}$  (Fig. 3 left) and  $\text{LiNO}_3$ :  $T_1 = 12$  s and for  ${}^6\text{LiI}$ :  $T_1 = 67.7$  s (Fig. 3 right) in  $\text{H}_2\text{O}$ . Therefore,  ${}^6\text{LiI}$  is the best option of the investigated compounds for storing

the hyperpolarized  ${}^6\text{Li}$ . As expected the relaxation times are shorter in proton containing (except for  ${}^6\text{LiI}$ ) solutions due to the increased dipolar coupling interaction. Due to the weak signal and decreasing signal intensity with decreasing concentration, only NMR measurements of three different concentrations were performed. Regarding the concentration dependence of the  $T_1$  relaxation times of the  ${}^6\text{Li}$ -salt samples we found the following:

As a reference,  $T_1$  of the reaction products of  ${}^6\text{Li}$  with water ( ${}^6\text{LiOD}$  in  $\text{D}_2\text{O}$  and  ${}^6\text{LiOH}$  in  $\text{H}_2\text{O}$ ) were measured (solubility  ${}^6\text{LiOD}/{}^6\text{LiOH} = 2.9$  mol/L [25]). These measurements are used to determine the influence of anions ( $\text{NO}_3^-$ ,  $\text{I}^-$ ,  $\text{Cl}^-$ ) on  $T_1$  of the  ${}^6\text{Li}$  ions. Due to the low solubility (spin density)  $T_1$  of just one dilution was measured. In Table 1, the measured  $T_1$  times of all samples are given for different concentrations. The data shows that  $T_1$  of  ${}^6\text{Li}$  salts in all  $\text{H}_2\text{O}$  salt solutions (except  ${}^6\text{LiI}$ ) are shorter than in  $\text{D}_2\text{O}$ . This behavior can be explained as follows.

In the case of the  ${}^6\text{Li}$  in liquids two spin–lattice relaxation rates are responsible for the main part of the relaxation rate [23]:

**Table 1**Longitudinal relaxation times of different concentrations and spin densities of  ${}^6\text{LiCl}$ ,  ${}^6\text{LiNO}_3$ ,  ${}^6\text{LiOD}$ ,  ${}^6\text{LiOH}$  and  ${}^6\text{LiI}$  in  $\text{H}_2\text{O}$  and  $\text{D}_2\text{O}$  at  $B_0 = 3.5 \text{ mT}$ .

${}^6\text{Li}$ -sample	Concentration (mol/L)	Spin density [ ${}^6\text{Li}$ ] in ( $\text{cm}^{-3}$ )	$T_1$ in $\text{D}_2\text{O}$ (s)	$T_1$ in $\text{H}_2\text{O}$ (s)
${}^6\text{LiCl}$	$C_{6\text{Li}} = 20.05$	$6.02 \times 10^{21}$	11.7	$\sim 1$
	$C_{6\text{Li}} = 16.96$	$5.1 \times 10^{21}$	17.3	
	$C_{6\text{Li}} = 9.75$	$2.9 \times 10^{21}$	37.6	
${}^6\text{LiNO}_3$	$C_{6\text{Li}} = 7.67$	$2.3 \times 10^{21}$	23.2	12.8
	$C_{6\text{Li}} = 6.35$	$1.9 \times 10^{21}$	34.1	23.7
	$C_{6\text{Li}} = 5.00$	$1.5 \times 10^{21}$	43.4	41.1
${}^6\text{LiI}$	$C_{6\text{Li}} = 11.13$	$3.3 \times 10^{21}$	67.3	67.7
	$C_{6\text{Li}} = 7.67$	$2.3 \times 10^{21}$	77.0	49.6
	$C_{6\text{Li}} = 5.50$	$1.6 \times 10^{21}$	177.7	28.4
${}^6\text{LiOD}$	$C_{6\text{Li}} = 3.09$	$9.3 \times 10^{20}$	43.0	
	$C_{6\text{Li}} = 1.85$	$5.5 \times 10^{20}$	55.8	
${}^6\text{LiOH}$	$C_{6\text{Li}} = 3.09$	$9.3 \times 10^{20}$		29.0
	$C_{6\text{Li}} = 1.85$	$5.5 \times 10^{20}$		58.1

### 1. The dipole–dipole interaction:

$$\left(\frac{1}{T_1}\right)_{6\text{Li}}^{\text{D,H}} \sim \rho_{6\text{Li}}^0 = \frac{8}{3} \cdot \frac{\gamma_{\text{D(H)}}^2 \cdot \gamma_{6\text{Li}}^2 \cdot h^2 \cdot \tau_c}{r_{\text{D(H)}6\text{Li}}^6} \quad (2)$$

Since the measurement takes place in the low frequency range ( $\omega = 2\pi \cdot 20 \text{ kHz}$ ), the “short correlation limit” ( $\omega\tau_c \ll 1$ ) is always valid.

Here the gyromagnetic ratio of deuterium (protons) and  ${}^6\text{Li}$  are  $\gamma_{\text{D(H)}}$  and  $\gamma_{6\text{Li}}$ .  $\omega_{\text{D,H}}$  and  $\omega_{6\text{Li}}$  are the angular frequencies of deuterium (protons) and  ${}^6\text{Li}$ .  $r_{\text{D(H)}6\text{Li}}$  is the average distance between both interaction partners and  $\tau_c$  the correlation time. The gyromagnetic ratio of  ${}^1\text{H}$  ( $\gamma_{\text{H}} = 42.75 \text{ MHz/G}$ ) is much larger than  $\text{D}$  ( $\gamma_{\text{D}} = 6.53 \text{ MHz/T}$ ). Thus,  $T_1$  of  ${}^6\text{Li}$  in  $\text{H}_2\text{O}$  is shorter than in  $\text{D}_2\text{O}$ .

2. For nuclei with  $I > 1/2$  the quadrupole interaction gives rise to an additional relaxation pathway with the spin–lattice relaxation rate  $(1/T_1)_Q$ . The interaction of the nuclei with quadrupole moment  $Q$  with fluctuating electric field gradients in its environment [24] is of the form:

$$\left(\frac{1}{T_1}\right)_Q \approx \frac{3}{4} \cdot \frac{2I_{6\text{Li}} + 3}{I_{6\text{Li}}^2(2I_{6\text{Li}} - 1)} \cdot \left(\frac{eQ}{h}\right)^2 \cdot \frac{\partial^2 V}{\partial z^2} \cdot \tau_q \quad (3)$$

$\frac{\partial^2 V}{\partial z^2}$  is the electric field gradient at the location of the core,  $\tau_q$  the correlation time of the quadrupolar interaction and  $I$  the spin quantum number of the  ${}^6\text{Li}$  nucleus ( $I_{6\text{Li}} = 1$ ). A further observation is that the  ${}^6\text{Li}$  longitudinal relaxation time in both solutions ( $\text{D}_2\text{O}$  and in  $\text{H}_2\text{O}$ ) becomes longer upon dilution (except for  ${}^6\text{LiI}$  in  $\text{H}_2\text{O}$ ) (Fig. 4). This is a result of the fact that for both dipole–dipole interaction and the

quadrupolar interaction the correlation time ( $\tau_c, \tau_q$ ) between  ${}^6\text{Li}$ -ions and the protons, deuterons and anions becomes shorter. Another reason for the  $T_1$  extension is, that at low  ${}^6\text{Li}$  concentrations each  ${}^6\text{Li}$ -ion is surrounded by six- $\text{H}_2\text{O}$  (or  $\text{D}_2\text{O}$ ) molecules, which are strongly bound to the  ${}^6\text{Li}$ -ion and thus forming a stable hydrate. Therefore, the  ${}^{35}\text{Cl}^-$ ,  ${}^{127}\text{I}^-$ ,  ${}^{14}\text{NO}_3^-$  anions cannot approach the  ${}^6\text{Li}$ -ion as close as the protons or deuterons. At high concentrations (e.g.  $\text{LiCl}$  in  $\text{H}_2\text{O}$ ,  $[{}^6\text{Li}^+] = 6.02 \times 10^{21} \text{ cm}^{-3}$  and  $[\text{H}_2\text{O}] = 1.6 \times 10^{22} \text{ cm}^{-3}$ ) there are not enough water molecules present to form the hexahydrate-complex, so that on average every  ${}^6\text{Li}$  has at least 3.2 anion contacts. Under these conditions, the  ${}^6\text{Li}$ -ions are strongly associated with the anions, which leads to long correlation times and a very short  $T_1$  ( $\sim 1 \text{ s}$ ) as a result of intense dipolar, quadrupolar and spin-rotation interaction.

As mentioned before, it is remarkable that  $T_1$  for  ${}^6\text{LiI}$  in  $\text{H}_2\text{O}$  exhibits a totally different behavior compared to the other solutions.  $T_1$  becomes shorter with decreasing concentration:  $T_1(11.3 \text{ mol}) = 67.7 \text{ s} > T_1(7.67 \text{ mol}) = 49.6 \text{ s} > T_1(5.5 \text{ mol}) = 28.4 \text{ s}$  (see Table 1).  $T_1$  of the  ${}^6\text{LiI}$  samples in  $\text{H}_2\text{O}$  approach the relaxation time of the  ${}^6\text{LiOH}$ -reference upon dilution of the samples (see Fig. 5) until a threshold is reached and  $T_1$  increases upon further dilution of the sample.

A possible explanation for this phenomenon is as follows: the dissolution process of  ${}^6\text{LiI}$  in  $\text{H}_2\text{O}$  is associated with an exothermic reaction leading to sample heating:

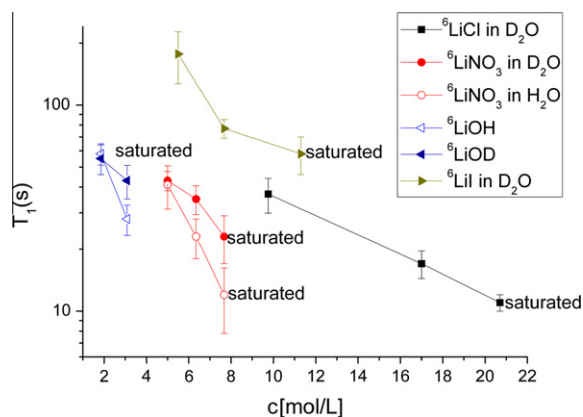
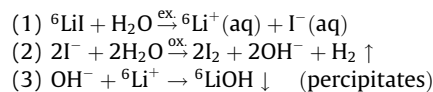


**Fig. 4.**  $T_1$ -relaxation time of all  ${}^6\text{Li}$ -samples as a function of concentration of the  ${}^6\text{Li}$ -salts in  $\text{D}_2\text{O}$  and  $\text{H}_2\text{O}$ . With decreasing concentration of the  ${}^6\text{Li}$ -salts  $T_1$  increases.

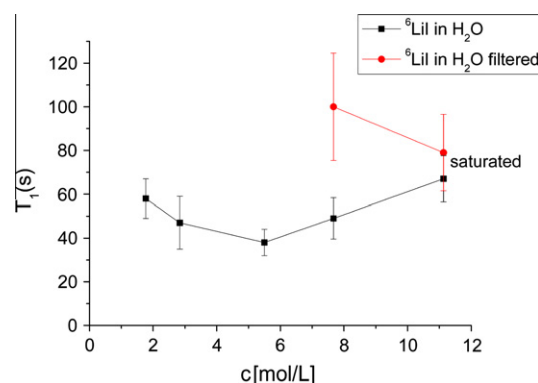


**Fig. 5.** Magnetization time of  ${}^6\text{LiI}$  in  $\text{H}_2\text{O}$ : the relaxation time  $T_1$  of  ${}^6\text{Li}$  is plotted as a function of concentration of  ${}^6\text{LiI}$  solution sample with precipitation (rectangle) and a filtered sample without precipitation (circle).

In this process  ${}^6\text{LiOH}$  is formed and due to its lower solubility compared to the iodide compound it settles as a precipitate at the bottom of the sample. Upon dilution the  ${}^6\text{LiOH}$  sediment dissolves and leads to above mentioned tendency. Until the threshold is reached the concentration of the  ${}^6\text{LiOH}$  solution is constant due to dilution of the precipitate and eventually, the  ${}^6\text{LiOH}$  is completely dissolved. From the threshold ( $c_{\text{LiI}} = 5.5 \text{ mol/L}$ ), any further dilution of the sample leads to a decreasing  ${}^6\text{Li}$  ion concentration and prolonged  $T_1$ . This was proven by removing the precipitate and diluting the sample showing the expected  $T_1$  prolongation when reducing the concentration (Fig. 5).

After the precipitate has been completely dissolved further dilution of the sample ( $c_{\text{LiI}} = 2.84 \text{ mol/L}$  and  $c_{\text{LiI}} = 1.77 \text{ mol/L}$ ) leads to a longer longitudinal relaxation time of  ${}^6\text{Li}$ . This corresponds to the behavior of all investigated  ${}^6\text{Li}$  samples. These results show that indeed the  ${}^6\text{LiOH}$  precipitate in the dilution leads to a shortening of the  ${}^6\text{Li}$  relaxation time. It is remarkable that this behavior could not be observed in case of  ${}^6\text{LiI}$  in  $\text{D}_2\text{O}$ , where regular concentration dependency was observed. We assume that this is a result of reduced dipole–dipole interaction due to the smaller gyromagnetic ratio of  ${}^2\text{D}$  that leads to a lower relaxation ratio and hence plays a less significant role.

#### 4. Conclusion

Our investigations of different lithium ion solutions in low magnetic fields ( $B_0 = 3.5 \text{ mT}$ ), show that the pre-polarized  ${}^6\text{Li}$  ( $B_p = 2 \text{ T}$ ) of the  ${}^6\text{LiI}$  salt solution in deuterated water ( $\text{D}_2\text{O}$ ) has the longest  $T_1$  (177 s). According to the presented results, hyperpolarized  ${}^6\text{LiI}$  salt solution provides an opportunity to maintain the polarization for a few minutes and measure the  ${}^6\text{Li}$  signal in low magnetic fields. By diluting the solution the relaxation time  $T_1$  of all  ${}^6\text{Li}$  salts increases with decreasing concentration. In the case of  ${}^6\text{LiI}$  in  $\text{H}_2\text{O}$  an inverse behavior was observed which occur due to formation of  ${}^6\text{LiOH}$  upon the solution of  ${}^6\text{LiI}$  in  $\text{H}_2\text{O}$ , which settles as a precipitate.  $T_1$  measurements of the  ${}^6\text{Li}$  salts in low-fields provide an important empirical data for future  ${}^6\text{Li}$  hyperpolarization studies. In future, hyperpolarized lithium ion salts could be used as contrast agents in clinical MRI because of the long relaxation times or to study transportation and reaction phenomena in lithium ion batteries.

#### References

- [1] A. Abragam, *The Principles of Nuclear Magnetism*, Clarendon Press, Oxford, 1961.
- [2] R.R. Ernst, G. Bodenhausen, A. Wokaun, *Principles of Nuclear Magnetic Resonance in One and Two Dimensions*, Clarendon Press, Oxford, 1987.

- [3] B. Blümich, *Essential NMR*, Springer Verlag, Berlin Heidelberg, 2005.
- [4] F. Bloch, W.W. Hansen, M. Packard, Nuclear induction, *Phys. Rev.* 69 (1946) 127.
- [5] T. Pietraß, H.C. Gaede, A. Bifone, A. Pines, J.A. Ripmeester, Monitoring xenon clathrate hydrate formation on ice surfaces with optically enhanced  ${}^{129}\text{Xe}$  NMR, *J. Am. Chem. Soc.* 117 (1995) 7520–7525.
- [6] H.W. Long, H.C. Gaede, J. Shore, L. Reven, C.R. Bowers, J. Kritzenberger, T. Pietraß, A. Pines, High-field cross polarization NMR From laser-polarized xenon to a polymer surface, *J. Am. Chem. Soc.* 115 (1993) 8491–8492.
- [7] H.C. Gaede, Y.-Q. Song, R.E. Taylor, E. J. Munson, J.A. Reimer, A. Pines, High-field cross polarization NMR from laser-polarized xenon to surface nuclei, *Appl. Magn. Reson.* 8 (1995) 373.
- [8] R.B. van Heeswijk, K. Uffmann, A. Comment, F. Kurdzesau, C. Perazzolo, C. Cudalbu, S. Jannin, J.A. Konter, Patrick, Hautle, B. van den Brandt, G. Navon, J. van der Klink, R. Gruetter, Hyperpolarized lithium-6 as a sensor of nanomolar contrast agent, *Magn. Reson. Med.* 61 (2009) 1489–1493.
- [9] W. Happer, Optical pumping, *Rev. Mod. Phys.* 44 (1972) 169–249.
- [10] S. Appelt, A.B. Baranga, C.J. Erickson, M.V. Romalis, A.R. Young, W. Happer, Theory of spin-exchange optical pumping of  ${}^3\text{He}$  and  ${}^{129}\text{Xe}$ , *Phys. Rev. A* 58 (1998) 1412–1439.
- [11] A. Abragam, M. Goldman, Principles of dynamic nuclear polarisation, *Rep. Prog. Phys.* 41 (1978) 395–467.
- [12] M.E. Halse, P.T. Callaghan, A dynamic nuclear polarization strategy for multi-dimensional Earth's field NMR, *J. Magn. Reson.* 195 (2008) 162–168.
- [13] M.D. Lingwood, I.A. Ivanov, A.R. Cote, S.J. Han, Heisenberg spin exchange effects of nitroxide radicals on Overhauser dynamic nuclear polarization in the low field limit at 1.5 mT, *J. Magn. Reson.* 204 (2010) 56–63.
- [14] G. Navon, Y.Q. Song, T. Room, S. Appelt, R.E. Taylor, A. Pines, Enhancement of solution NMR and MRI with laser-polarized Xenon, *Science* 271 (1996) 1848–1851.
- [15] S. Appelt, F.W. Häsing, S. Bear-Lang, N.J. Shah, B. Blümich, Proton magnetization enhancement of solvents with hyperpolarized xenon in very low-magnetic fields, *Chem. Phys. Lett.* 348 (2001) 263.
- [16] R.W. Adams, J.A. Aguilar, K.D. Atkinson, M.J. Cowley, I. Paul, P. Elliott, S.B. Duckett, G.G.R. Green, I.G. Khazal, J. López-Serrano, D.C. Williamson, Reversible interaction with para-hydrogen enhance NMR sensitivity by polarization transfer, *Science* 323 (2009) 1708–1711.
- [17] S.B. Duckett, N.J. Wood, Parahydrogen-based NMR methods as a mechanistic probe in inorganic chemistry, *Coord. Chem. Rev.* 252 (2008) 278–291.
- [18] C. Russell Bowers, D.P. Weitekamp, Transformation of symmetrization order to nuclear-spin magnetization by chemical reaction and nuclear magnetic resonance, *Phys. Rev. Lett.* 57 (1986) 11270–11275.
- [19] K. Golman, R. Zandt, M. Thanning, Real-time metabolic imaging, *Proc. Natl. Acad. Sci. USA* 103 (2006) 11270–11275.
- [20] P. Bhattacharya, K. Harris, A.P. Lin, M. Manson, V.A. Norton, W.H. Perman, D.P. Weitekamp, B.D. Ross, Ultra-fast three dimensional imaging of hyperpolarized  ${}^{13}\text{C}$  in vivo, *MAGMA* 18 (2005) 245–256.
- [21] S. Appelt, S. Glögler, F.W. Häsing, U. Sieling, A. Gordji-Nejad, B. Blümich, NMR spectroscopy in the milli-Tesla regime: measurement of  ${}^1\text{H}$  chemical-shift difference below the line width, *Chem. Phys. Lett.* 485 (2010) 217–220.
- [22] A.G. Webb, Radiofrequency microcoils in magnetic resonance, *Prog. Nucl. Magn. Reson. Spectrosc.* 31 (1997) 1–42.
- [23] F.W. Wehrli, Spin–lattice relaxation of some less common weakly quadrupolar nuclei, *J. Magn. Reson.* 30 (1978) 193–209.
- [24] H.G. Hertz, R. Tusch, N.S. Bowman, Intermolecular and intramolecular motions in the solvation spheres of some ions in methyl and ethyl alcohol, *J. Phys. Chem.* 80 (1976).
- [25] D.R. Lide, *CRC Handbook of Chemistry and Physics*, 87th ed., CRC Press, Boca Raton, FL, 2006.